

## ■ UPPER LIMB

# Effects of focused continuous pulsed electromagnetic field therapy on early tendon-to-bone healing

## RAT SUPRASPINATUS DETACHMENT AND REPAIR MODEL



**O. Dolkart,  
E. Kazum,  
Y. Rosenthal,  
O. Sher,  
G. Morag,  
E. Yakobson,  
O. Chechik,  
E. Maman**

From Tel Aviv Sourasky Medical Center, Sackler Faculty of Medicine, Tel Aviv University, Tel Aviv, Israel

### Aims

Rotator cuff (RC) tears are common musculoskeletal injuries which often require surgical intervention. Noninvasive pulsed electromagnetic field (PEMF) devices have been approved for treatment of long-bone fracture nonunions and as an adjunct to lumbar and cervical spine fusion surgery. This study aimed to assess the effect of continuous PEMF on postoperative RC healing in a rat RC repair model.

### Methods

A total of 30 Wistar rats underwent acute bilateral supraspinatus tear and repair. A miniaturized electromagnetic device (MED) was implanted at the right shoulder and generated focused PEMF therapy. The animals' left shoulders served as controls. Biomechanical, histological, and bone properties were assessed at three and six weeks.

### Results

Extension of the tendon from preload to the maximum load to failure was significantly better in the PEMF-treated shoulders at three weeks compared to controls ( $p = 0.038$ ). The percentage strain was significantly higher in the PEMF group at both timepoints ( $p = 0.037$ ). Collagen organization was significantly better ( $p = 0.034$ ) as was tissue mineral density in the PEMF-treated group at three weeks ( $p = 0.028$ ). Tendon immunohistochemistry revealed a prominent increase in type I collagen at the repair site at three weeks following continuous PEMF treatment compared with controls. None of the other tested parameters differed between the groups.

### Conclusion

MED-generated PEMF may enhance early postoperative tendon-to-bone healing in an acute rat supraspinatus detachment and repair model. Superior biomechanical elasticity parameters together with better collagen organization suggest improved RC healing.

**Cite this article:** *Bone Joint Res* 2021;10(5):298–306.

**Keywords:** Pulsed electromagnetic field therapy, Supraspinatus repair, Rotator cuff, Tendon-to-bone healing

### Article focus

- This study addresses the effects of the continuous pulsed electromagnetic field (PEMF) on rotator cuff (RC) healing in a rat model.
- It was hypothesized that PEMF administration following RC detachment and repair would have positive effects on the following outcomes: biomechanical properties; repaired tissue morphology

including tenocytes, collagen, and vascularity; and glenoid bone density.

### Key messages

- PEMF application may have a positive effect on early stages of RC healing in rats.
- Specifically, superior biomechanical elasticity parameters, together with better collagen organization, were found in

Correspondence should be sent to Oleg Dolkart; email: [dolkarto@gmail.com](mailto:dolkarto@gmail.com)

doi: 10.1302/2046-3758.105.BJR-2020-0253.R2

*Bone Joint Res* 2021;10(5):298–306.

miniaturized electromagnetic device (MED)-treated groups compared to controls.

- Additionally, improvements in collagen I expression were identified with PEMF treatment.

### Strengths and limitations

- The rat model used in this study is valid and commonly used to study RC healing.
- An acute model of RC injury does not accurately mimic the chronic, degenerative age-related RC tears seen in humans.
- RC repair method used in this model is different from that employed in humans (e.g. open surgery vs arthroscopic surgery, type of sutures, suture technique).

### Introduction

Rotator cuff (RC) tears constitute a widespread problem that causes substantial pain and disability, with an incidence of 80% among people aged 70 years or older.<sup>1,2</sup> Although the clinical outcome of RC repair is generally favourable, postoperative re-tear or failure to heal still remain major concerns, with an incidence up to 25%.<sup>3,4</sup> A repaired tendon and a repaired tendon-to-bone interface present inferior tissue properties compared to an uninjured RC tendon. The newly formed tissue is mostly fibrotic and disorganized, and it reattaches poorly to the bone.

Many noninvasive therapeutic devices have been used postoperatively to improve tendon-to-bone healing, including therapeutic ultrasound and shock-wave therapy.<sup>5,6</sup> Noninvasive devices that emit pulsed electromagnetic fields (PEMFs) have been approved by the Food and Drug Administration (FDA) for the treatment of long-bone fracture nonunions, and as an adjunct to lumbar and cervical spine fusion surgery.<sup>5,7-12</sup> About four decades ago, researchers found that PEMF therapy could be practical to accelerate wound healing and fracture repair, reduce haematoma, treat soft-tissue injuries, and alleviate inflammation.<sup>13</sup> Current data on the potential influence of PEMF on tendon and tendon-to-bone healing, however, are scarce.

Several preclinical studies have examined the effect of PEMF in various biological models, including one study on the effect of PEMF in a rat fibular osteotomy model, which found increased bone callus volume, stiffness, and modulus in the PEMF-treated group.<sup>14</sup> Because PEMF therapy is commonly used in bone fracture healing, it has been considered that there may be a potential therapeutic application of PEMF therapy to enhance soft-tissue healing as well.<sup>15</sup> Preclinical studies examining tendon-to-tendon healing have also suggested that PEMF increases tensile strength of a repaired Achilles transection in a rat model.<sup>16</sup> A recent study by Tucker et al<sup>17</sup> indicated that PEMF improved early tendon-to-bone healing without altering joint

function in a rat RC repair model, but the animals were exposed to a systemic PEMF signal.

The miniaturized electromagnetic device (MED) (Magdent Ltd, Israel) is shaped like a dental healing abutment. It houses microelectronic modules that generate PEMF to improve bone formation after a dental implant procedure. That system was developed based on positive results observed in other bone-healing models, but it uses conceptually similar systems that require an external power source and wiring, making this option inconvenient and cumbersome.

The objective of the current study was to evaluate the effects on tendon-to-bone healing of a new PEMF-generating device that was implanted at the site of RC repair. It was hypothesized that PEMF administration following RC detachment and repair would have positive effects on the following outcomes: biomechanical properties; repaired tissue morphology including tenocytes, collagen, and vascularity; and glenoid bone density. The healing was assessed by biomechanical, micro-CT ( $\mu$ CT), and histological results of its application.

### Methods

**Animals.** All procedures were approved by the Institutional Animal Care and Use Committee at the Tel Aviv Sourasky Medical Center. A total of 30 adult male Wistar rats (250 g to 300 g body weight) were used for the experiments. The animals were maintained on a 12-hour light/12-hour dark cycle at 21°C to 22°C and acclimatized for seven days before the experiments were initiated. The rats were allowed ad libitum access to food and water. An ARRIVE checklist is included in the Supplementary Material to show that the ARRIVE guidelines were adhered to in this study.

**RC repair model.** All the animals were subjected to identical bilateral supraspinatus detachment and repair as described,<sup>18</sup> and all surgeries were performed under isoflurane-induced general anaesthesia. Surgical exposure of the supraspinatus tendon was achieved as follows under aseptic operating room protocols. A 2 cm skin incision was performed over the cranial aspect of the glenohumeral joint in a deltoid split approach. Medial and lateral flaps were raised to expose the deltoid muscle. The deltoid muscle was partially detached from the posterior acromion, split distally for a distance of 1 cm to 1.5 cm, and retracted with a pointed towel clamp to expose the underlying supraspinatus tendon. A tag suture was applied to the supraspinatus, and the tendon was sharply detached at its insertion on the greater tuberosity. The supraspinatus tendon's footprint on the surface of the greater tuberosity was gently debrided with a scalpel to enhance tendon-to-bone healing. A Mason-Allen stitch was placed into the supraspinatus tendon (4 to 0 Ethibond; Johnson & Johnson, USA) and then passed through a bone tunnel in the greater tuberosity.

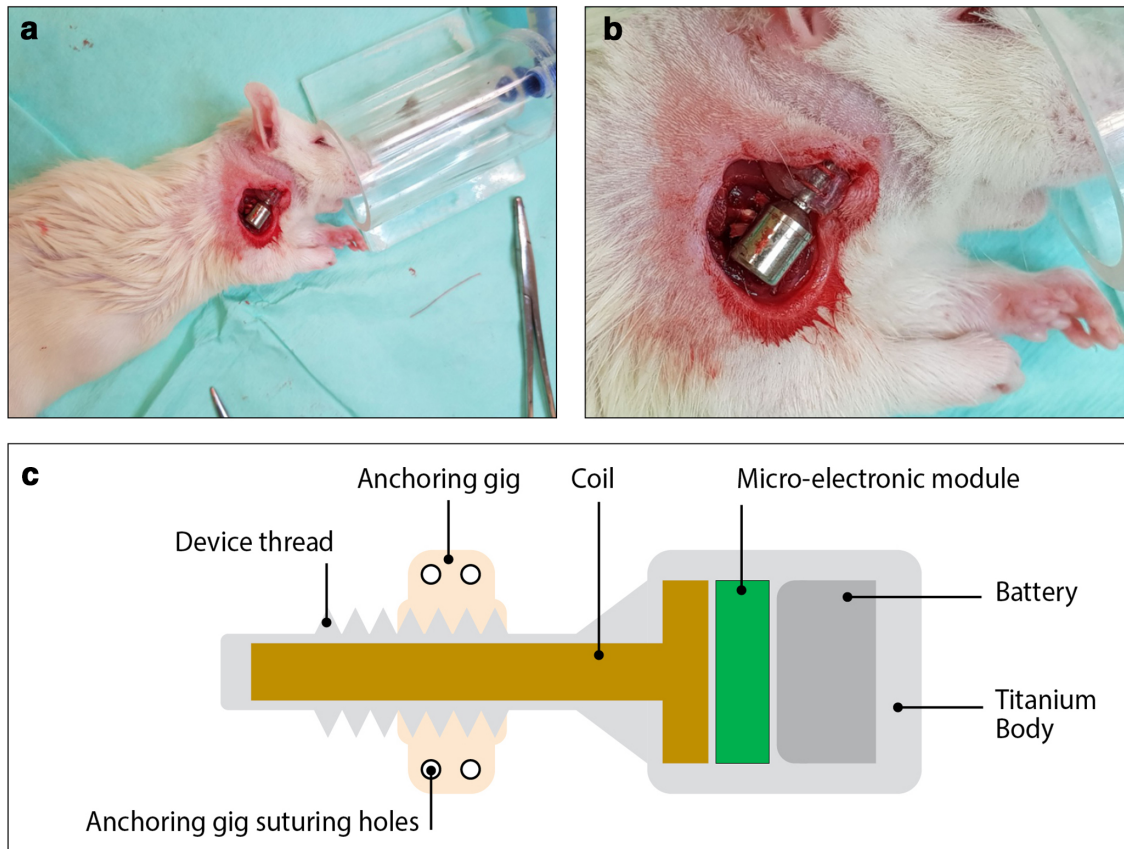


Fig. 1

a) and b) Miniaturized electromagnetic device (MED) implantation procedure in the subcutaneous space on the right shoulder. c) Schematic presentation of the MED-pulsed electromagnetic field (PEMF) generating device. The device is shaped like a dental healing abutment and made of a titanium body that houses a microelectronics module, micro battery, and coil.

Gross evaluation of the tissue immediately after repair revealed good apposition of the tendon onto the bone, with no visible gap. The MED was implanted in a subcutaneous space at the right shoulder and secured with sutures following the tendon repair (Figure 1). The skin was closed by nonabsorbable skin sutures.

**MED device description.** The MED is a miniature PEMF generator. The device is shaped like a dental healing abutment and made of a titanium body that houses inside a microelectronics module, micro battery, and coil. The device is manufactured with an external thread on its lower part. In order to anchor the device in place during RC repair surgery in rats, a plastic gig was manufactured, which had an internal thread and designated suturing holes at its limbs. The MED device was connected to the gig by threading it into the gig, and during the procedure it was sutured over the connection area through the designated suturing holes, thus keeping the MED device in place during the follow-up (FU) period (Figure 1).

**PEMF description.** The MED generates a PEMF, operating continuously for up to 40 days. The PEMF outside the titanium body is effective at a distance of up to 3 mm. The specific parameters of the PEMF are: intensity

– varies depending on the positioning of the device relative to the tissue target area, and ranges between 0.05 mT to 0.5 mT; and frequency – 10 kHz. The device operates continuously at the same parameters during the entire duration of treatment.

**External measuring probe description.** In order to verify that the MED devices are operating properly during the study period, an external probe was designed and used. The probe is made of a plastic housing, incorporating sensitive micro coils, connected to output wires, which are connected to an oscilloscope. In order to verify the operation of the MED devices during the trial, the probe was placed externally on the rat skin, over the device location, and the PEMF parameters were checked on the oscilloscope.

To eliminate the variance in PEMF intensity, due to different distances between the implanted MED device and the external probe in each animal, immediately after the MED device implantation and suturing of the rat's skin, a baseline measurement was taken using the external probe. This was used for comparison, with measurements taken once a week during the entire FU period.

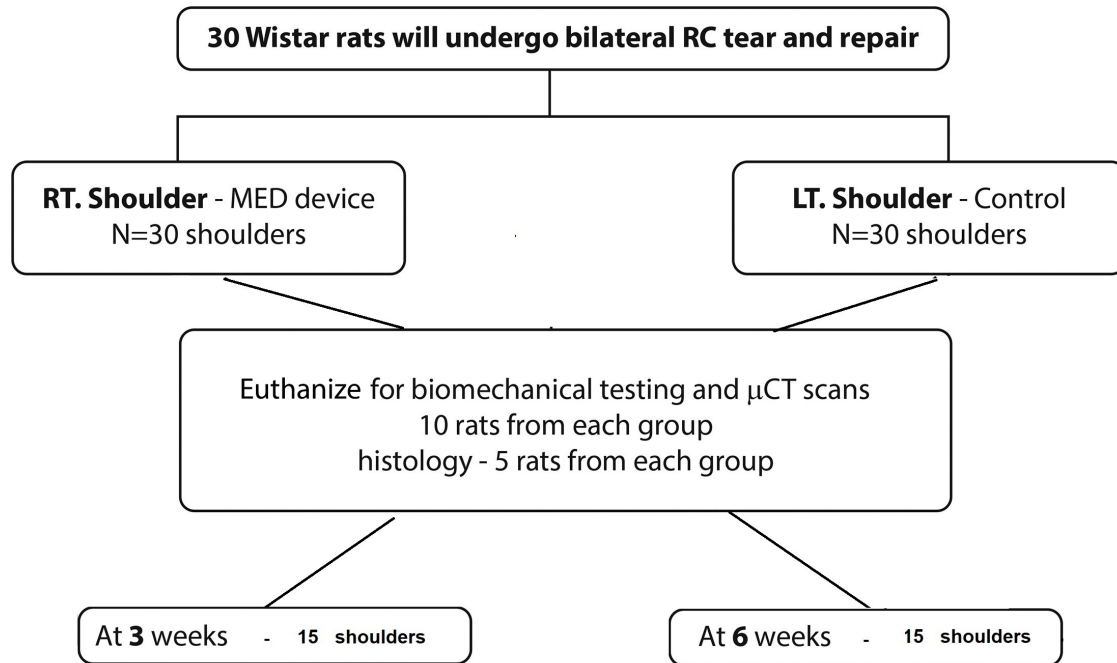


Fig. 2

Study flowchart showing biomechanical, histological, and osseous properties assessed at three and six weeks. LT, left; MED, miniaturized electromagnetic device; RC, rotator cuff; RT, right;  $\mu$ CT, micro-CT.

**Outcome parameters assessment.** Biomechanical, histological, and osseous properties were assessed at three and six weeks (Figure 2).

**Biomechanical testing.** The humerus and supraspinatus tendon specimens were harvested and dissected free of surrounding tissue. The supraspinatus tendons were kept in saline solution at room temperature, thus preventing necrosis and dehydration. All biomechanical tests were performed on the same day as rat euthanasia. In all specimens, the suture used to repair the tendon to its footprint was removed in cases where it was completely loose, in order not to disturb the surrounding healing tissue. Digital calipers were used to measure the cross-sectional area of the supraspinatus tendon at the point of insertion into the humerus as previously described.<sup>19</sup> The humerus was attached directly to the clamp in position of 45° angle to direct the pulling force in the original direction of the supraspinatus. The tendon was secured in a clamp by sandpaper, and a Lloyd materials testing machine was used to complete the biomechanical testing (Model LS5; Lloyd Instruments, UK). Tests were performed with YLC-0100-A1 0.5% accuracy 100 N loadcell (Lloyd Instruments). The biomechanical testing protocol was previously established by Galatz et al.<sup>20</sup> The tendons were subjected to a preload of 0.2 N, five preconditioning cycles to 0.38 mm displacement, 300 seconds of a stress relaxation test at 0.38 mm displacement, and 300 seconds of recovery. Specimens were subsequently pulled to failure at a rate of 0.5 mm/second. All samples failed at the repair site.

Biomechanical data collection and analyses were performed with Nexygen Plus Software Version 4.0.1 (Lloyd Instruments).

**$\mu$ CT scanning.** Bone density was assessed by  $\mu$ CT scanning (Xradia Micro-CT X-ray Tomographical Microscope; Zeiss, Germany). The humeri samples were maintained in a medium of 4% neutral buffered formalin for 48 hours and then stored in 70% ethanol.  $\mu$ CT scans were performed at energy 90 kVp, tube intensity 200  $\mu$ A, integration time 1,000 msec, with an isotropic nominal resolution of 17.2  $\mu$ m. The region of interest was defined as the area 5 mm proximal from the growth plate, which included the greater tuberosity and the bony footprint. Bone mineral density (BMD), trabecular thickness (Tb, Th, mm), trabecular spacing (mm), tissue mineral density (TMD), bone volume (BV), and bone volume fraction (BV/total volume) were measured.

**Histological analysis.** Histological analyses were performed to assess cell shape, cellularity, and collagen fibre organization at the injury site of the repaired supraspinatus tendon. The site of injury was defined as the central portion of the fibrous scar tissue. The supraspinatus-humerus units of the euthanized animal were dissected, fixed in formalin, and processed by standard paraffin techniques. Next, 7  $\mu$ m sections were then stained with haematoxylin and eosin (H&E) and Masson's trichrome (MT). A blinded musculoskeletal pathologist (OS) evaluated the tissue sections from the repair site for tenocytes, collagen, and vascularity under light and polarized light microscopy (Nikon Eclipse TS100; Nikon Instruments Europe BV, The Netherlands) using the semiquantitative

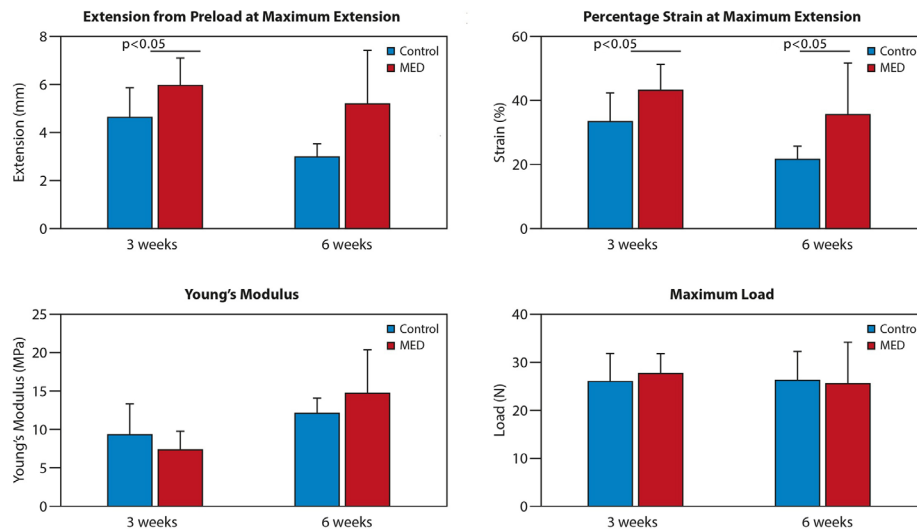


Fig. 3

Biomechanical testing results. Elongation of the tendon from preload to the maximum load to failure was significantly better in the pulsed electromagnetic field (PEMF)-treated animals at three weeks compared to the controls ( $p = 0.038$ , independent-samples  $t$ -test). The percentage strain was significantly higher in the PEMF group at both three- and six-week timepoints. Graphs are reported as mean and standard deviation (SD). \* $p < 0.05$  versus control group, independent-samples  $t$ -test. MED, miniaturized electromagnetic device.

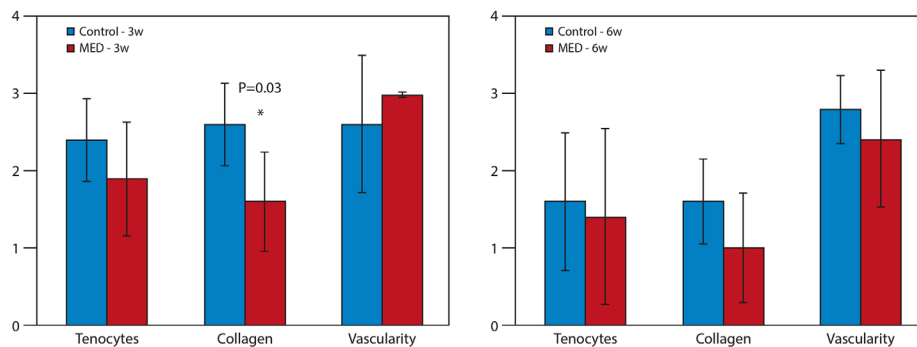


Fig. 4

Three parameters of the Bonar score, miniaturized electromagnetic device (MED) versus control. Collagen organization was significantly better in the pulsed electromagnetic field (PEMF)-treated group at three weeks ( $p = 0.034$ , independent-samples  $t$ -test). Collagen organization did not differ significantly between groups at six weeks ( $p = 0.101$ , Mann-Whitney U test). Graphs are mean and standard deviation (SD). \* $p < 0.05$  versus control group, independent-samples  $t$ -test.

Bonar score<sup>21</sup> in which 0 = normal appearance and 3 = a markedly abnormal appearance.

The following three criteria were evaluated: tenocytes, collagen organization, and vascularity. Each of these parameters was scored individually by a musculoskeletal pathologist (OS) using a scale of 0 to 3: when normal parameters were scored 0 and most pathological were scored 3.

**Tenocytes:** 0 – elongated nuclei with no obvious cytoplasm; 1 – ovoid nuclei with lesser cytoplasm; 2 – round nuclei with a small amount of cytoplasm; 3 – large, round nuclei with abundant cytoplasm.

**Collagen:** 0 – tightly arranged and well-demarcated bundles with polarization pattern with normal crimping; 1 – diminished fibre polarization: separation of individual fibres with maintenance of demarcated bundles; 2 – fibres separated with loss of demarcation of bundles

with loss of normal polarization; 3 – fibres markedly separated, loss of architecture.

**Vascularity:** 0 – blood vessels coursing between bundles; 1 – less than one cluster of capillaries per ten high-power field; 2 – one to two clusters of capillaries per ten high-power fields; 3 – more than two clusters per ten high-power fields.

Three sequential sections for each staining were evaluated from each specimen. Digital images were captured by an inverted microscope (Nikon Eclipse TS100).

**Tendon immunohistochemistry.** The immunohistochemistry analysis was performed by incubating the sections with specific antibodies for type I and type III collagen (Abcam, UK). Following deparaffinization and rehydration, sections underwent digestion and were blocked with 3% hydrogen peroxide to inhibit endogenous peroxidase activity, washed in phosphate-buffered saline

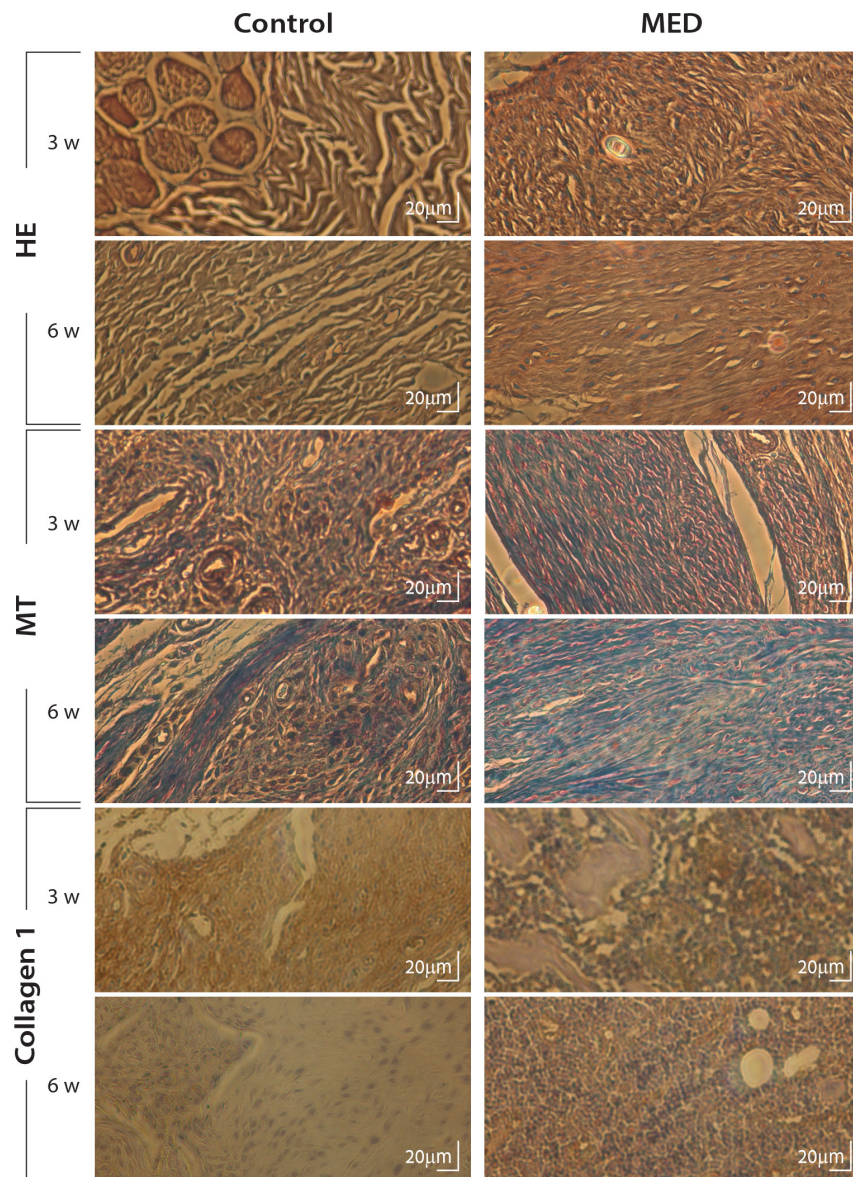


Fig. 5

Representative images of histological and immunohistochemical analyses. Miniaturized electromagnetic device (MED) and control groups were evaluated at three and six weeks. Tendon immunohistochemistry revealed a prominent increase in type I collagen at the repair site at three weeks following continuous pulsed electromagnetic field (PEMF) treatment compared with controls, but these differences were less notable after six weeks. HE, haematoxylin and eosin; MT, Masson's trichrome.

solution, blocked to prevent non-specific binding, and incubated with primary antibody. For type I collagen detection, section was then incubated with ab21287, 2 µg/ml (Abcam), for 15 minutes at room temperature and detected using a horseradish peroxidase (HRP)-conjugated compact polymer system. Type III collagen detection was performed by incubating the sections with ab7778 (Abcam) at a concentration of 1 µg/ml for 20 minutes. A total of five histological sections per antibody per time-point per group was evaluated. The slides were evaluated

at magnification  $\times 200$  and qualitatively assessed in a blinded fashion.

**Statistical analysis.** The power analysis was based on a previous study that assessed RC tendon healing in rats after interventions. A strength increase of 20% was set as clinically significant for the current study. With these evaluations for biomechanical testing, a power of 80% is achieved using ten animals per group with  $\alpha = 0.05$ . All statistical comparisons were made between the PEMF and control (non-PEMF) groups at the same timepoints.

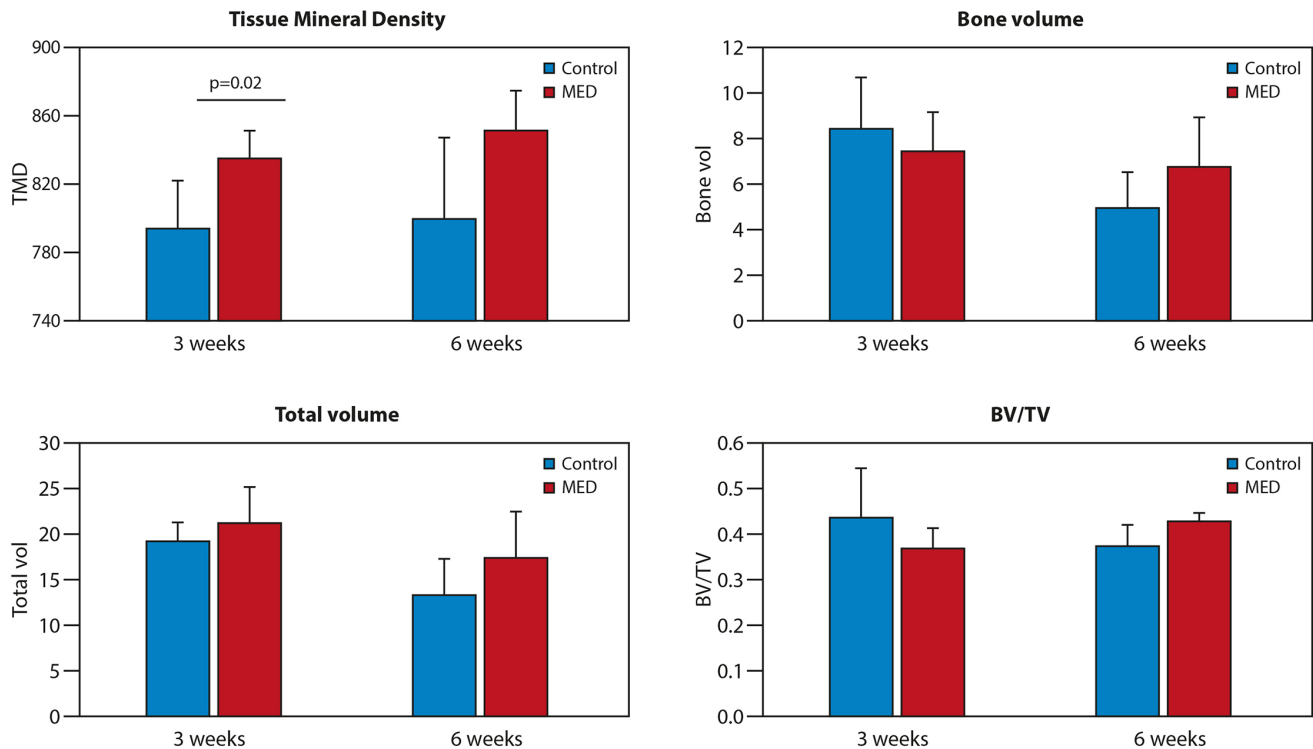


Fig. 6

Micro-CT results. Tissue mineral density was significantly higher in the pulsed electromagnetic field (PEMF)-treated group compared to controls at three weeks ( $p = 0.028$ ); the same trend was observed at six weeks, however this was not statistically significant ( $p = 0.120$ ). Graphs are reported as mean and standard deviation (SD). All  $p$ -values were calculated using independent-samples  $t$ -test. BV/TV, bone volume/total volume; MED, miniaturized electromagnetic device; TMD, tissue mineral density.

Mechanical testing,  $\mu$ CT, and collagen fibre organization comparisons were done using independent-samples  $t$ -tests with significance set at  $p < 0.05$ . Semiquantitative histological comparisons were performed using Mann-Whitney U tests with significance set at  $p < 0.05$ .

## Results

**General observations.** All rats demonstrated normal gait patterns and food consumption postoperatively. All RC repairs (PEMF-treated and control groups) were grossly intact at the time of euthanasia. There were no failed repairs or proximal humeral fractures. In addition, there were no signs of infection or significant injuries in any of the animals' shoulders.

**Biomechanical properties.** All specimens failed at the original tear site. Improvements in mechanical properties at both three and six weeks postoperative were identified in the PEMF-treated group compared with untreated animals. There were no statistically significant differences in relaxation over time within each group and between study groups (data not shown).

A significantly higher magnitude of elongation was presented in the PEMF-treated animals at three weeks compared to the controls ( $p = 0.05$ , independent-samples  $t$ -test) (Figure 3). The percentage strain was significantly

higher in the PEMF group at both three- and six-week timepoints. No statistically significant differences were found in maximal load, stiffness, and maximum stress at any timepoint (Figure 3).

**Histology.** No differences were found in tenocyte shape or vascularity between the PEMF-treated animals compared with the non-PEMF controls at any timepoint. Collagen organization was significantly better in the PEMF-treated group at three weeks ( $p = 0.034$ , Mann-Whitney U test). Collagen organization did not differ significantly between groups at six weeks ( $p = 0.101$ , Mann-Whitney U test) (Figures 4 and 5).

Tendon immunohistochemistry revealed a prominent increase in type I collagen at the repair site at three weeks following continuous PEMF treatment compared with controls, but these differences were less notable after six weeks (Figure 5).

**Micro-CT.** Tissue mineral density was significantly higher in the PEMF-treated group compared to controls at three weeks ( $p = 0.028$ , independent-samples  $t$ -test); the same trend was observed at six weeks as well, however this was not statistically significant ( $p = 0.120$ , independent-samples  $t$ -test). Bone volume was slightly higher in the PEMF-treated group at six weeks

( $p = 0.141$ , independent-samples  $t$ -test), while none of the other parameters differed between the groups (Figure 6).

## Discussion

The principal results of this study suggest that PEMF application may have a positive effect on early stages of RC healing in rats. Specifically, superior biomechanical elasticity parameters together with better collagen organization were found in MED-treated groups compared to controls. Additionally, improvements in collagen I expression were identified with PEMF treatment. There was no difference in maximal load to failure between the groups.

Two recently published studies examined the effects of systemically applied PEMF on RC healing in rats. Tucker et al<sup>17</sup> examined the effect of exposure of a commercially available and Food and Drug Administration (FDA)-approved PEMF waveform on tendon-to-bone healing in a rat RC model. In line with our current study results, they found that the PEMF group had a decreased cross-sectional area and increased modulus at four weeks, and that the PEMF group had increased modulus and more rounded cells in the midsubstance at eight weeks. Moreover, they found that the PEMF group had improved maximum stress at four weeks and bone quality at 16 weeks. Another study by the same research group investigated the influence of both PEMF frequency and exposure time on RC healing.<sup>22</sup> As observed in their previous study and similar to our current study, their later study demonstrated improvements in different mechanical properties at various endpoints for all treatment methods when compared with untreated animals, regardless of PEMF frequency or duration. Collagen organization improved for several of the treatment groups compared with controls. In addition, improvements in type I collagen and fibronectin expression were identified with PEMF treatment. Generally, the results of both of their studies suggested that PEMF therapy appears to have a positive effect on RC healing in rats.

Liu et al<sup>23</sup> examined the effects of PEMF on human tenocyte growth and differentiation in vitro. RC tissue was harvested from one healthy 19-year-old male donor. They showed a significant enhancement of tendon gene and growth factor expression tenocytes extracted from human RC tendons after two weeks of exposure to PEMF.

To the best of our knowledge, this is the first study to examine the effects on RC healing of an implanted device with internal PEMF stimulators. This device (MED) produces an electromagnetic field around the target site similar to that of external devices. The ability of MED-generated PEMF to improve bone healing had been demonstrated both in vivo and in clinical studies.<sup>24,25</sup> The advantage of this device is that the effective electromagnetic field is directed precisely around

the tendon-to-bone repair site and there is no need to use an external PEMF source. Thanks to the very small size of the MED (i.e. 22.5 mm), we were able to use it as a subcutaneous implant in a small animal model. This allows for continuous local activation of the PEMF device for 24 hours a day, with the goal of achieving improved healing in the early postoperative stage.

There are several limitations to this study. Although the rat model used in this study is valid and commonly used to study RC healing, it does not accurately mimic the chronic, degenerative age-related RC tears seen in humans. Additionally, because of the small size of the animal, the RC repair method used in our model is different from that employed in humans (e.g. open surgery vs arthroscopic surgery, type of sutures, suture technique). Finally, the effects of PEMF on RC healing were examined only at early postoperative timepoints.

Within the limitations of the present study, we conclude that MED-generated PEMF may enhance early postoperative tendon-to-bone healing in an acute rat supraspinatus detachment and repair model. Superior biomechanical elasticity parameters together with better collagen organization suggest improved RC healing.

## Supplementary material



ARRIVE checklist included to show that the ARRIVE guidelines were adhered to in this study.

## References

1. Yamaguchi K, Ditsios K, Middleton WD, Hildebolt CF, Galatz LM, Teefey SA. The demographic and morphological features of rotator cuff disease. A comparison of asymptomatic and symptomatic shoulders. *J Bone Joint Surg Am.* 2006;88-A(8):1699–1704.
2. Milgrom C, Schaffler M, Gilbert S, van Holsbeeck M. Rotator-cuff changes in asymptomatic adults. The effect of age, hand dominance and gender. *J Bone Joint Surg Br.* 1995;77-B(2):296–298.
3. Sobhy MH, Khater AH, Hassan MR, El Shazly O. Do functional outcomes and cuff integrity correlate after single- versus double-row rotator cuff repair? A systematic review and meta-analysis study. *Eur J Orthop Surg Traumatol.* 2018;28(4):593–605.
4. Wang Z, Li H, Long Z, et al. Biomechanical evaluation of a novel double rip-stop technique with medial row knots for rotator cuff repair: an in vitro study. *Bone Joint Res.* 2020;9(6):285–292.
5. Lovric V, Ledger M, Goldberg J, et al. The effects of low-intensity pulsed ultrasound on tendon-bone healing in a transosseous-equivalent sheep rotator cuff model. *Knee Surg Sports Traumatol Arthrosc.* 2013;21(2):466–475.
6. Springer J, Badgett RG. ACP Journal Club: optimized extracorporeal shock-wave therapy improved pain and functioning in chronic plantar fasciitis. *Ann Intern Med.* 2015;163(10):JC8.
7. Foley KT, Mroz TE, Arnold PM, et al. Randomized, prospective, and controlled clinical trial of pulsed electromagnetic field stimulation for cervical fusion. *Spine J.* 2008;8(3):436–442.
8. Garland DE, Moses B, Salyer W. Long-term follow-up of fracture nonunions treated with PEMFs. *Contemp Orthop.* 1991;22(3):295–302.
9. Goodwin CB, Brighton CT, Guyer RD, Johnson JR, Light KI, Yuan HA. A double-blind study of capacitively coupled electrical stimulation as an adjunct to lumbar spinal fusions. *Spine.* 1999;24(13):1349.
10. Linovitz RJ, Pathria M, Bernhardt M, et al. Combined magnetic fields accelerate and increase spine fusion: a double-blind, randomized, placebo controlled study. *Spine.* 2002;27(13):1383–1389.
11. Mooney V. A randomized double-blind prospective study of the efficacy of pulsed electromagnetic fields for interbody lumbar fusions. *Spine.* 1990;15(7):708–712.

12. **Coric D, Bullard DE, Patel VV, et al.** Pulsed electromagnetic field stimulation may improve fusion rates in cervical arthrodesis in high-risk populations. *Bone Joint Res.* 2018;7(2):124–130.
13. **Raji AR, Bowden RE.** Effects of high peak pulsed electromagnetic fields on degeneration and regeneration of the common peroneal nerve in rat. *Lancet.* 1982;2(8295):444–445.
14. **Midura RJ, Ibiwoye MO, Powell KA, et al.** Pulsed electromagnetic field treatments enhance the healing of fibular osteotomies. *J Orthop Res.* 2005;23(5):1035–1046.
15. **Uzunca K, Birtane M, Taştekin N.** Effectiveness of pulsed electromagnetic field therapy in lateral epicondylitis. *Clin Rheumatol.* 2007;26(1):69–74.
16. **Strauch B, Patel MK, Rosen DJ, Mahadevia S, Brindzei N, Pilla AA.** Pulsed magnetic field therapy increases tensile strength in a rat Achilles' tendon repair model. *J Hand Surg Am.* 2006;31(7):1131–1135.
17. **Tucker JJ, Cirone JM, Morris TR, et al.** Pulsed electromagnetic field therapy improves tendon-to-bone healing in a rat rotator cuff repair model. *J Orthop Res.* 2017;35(4):902–909.
18. **Dolkart O, Chechik O, Zarfati Y, Brosh T, Alhajjra F, Maman E.** A single dose of platelet-rich plasma improves the organization and strength of a surgically repaired rotator cuff tendon in rats. *Arch Orthop Trauma Surg.* 2014;134(9):1271–1277.
19. **Gulotta LV, Kovacevic D, Packer JD, Deng XH, Rodeo SA.** Bone marrow-derived mesenchymal stem cells transduced with scleraxis improve rotator cuff healing in a rat model. *Am J Sports Med.* 2011;39(6):1282–1289.
20. **Galatz LM, Sandell LJ, Rothermich SY, et al.** Characteristics of the rat supraspinatus tendon during tendon-to-bone healing after acute injury. *J Orthop Res.* 2006;24(3):541–550.
21. **Maffulli N, Longo UG, Franceschi F, Rabitti C, Denaro V.** Movin and Bonar scores assess the same characteristics of tendon histology. *Clin Orthop Relat Res.* 2008;466(7):1605–1611.
22. **Huegel J, Choi DS, Nuss CA, et al.** Effects of pulsed electromagnetic field therapy at different frequencies and durations on rotator cuff tendon-to-bone healing in a rat model. *J Shoulder Elbow Surg.* 2018;27(3):553–560.
23. **Liu M, Lee C, Laron D, et al.** Role of pulsed electromagnetic fields (PEMF) on tenocytes and myoblasts-potential application for treating rotator cuff tears. *J Orthop Res.* 2017;35(5):956–964.
24. **Barak S, Matalon S, Dolkart O, Zavan B, Mortellaro C, Piattelli A.** Miniaturized electromagnetic device abutment improves stability of the dental implants. *J Craniofac Surg.* 2019;30(4):1055–1057.
25. **Barak S, Neuman M, Iezzi G, Piattelli A, Perrotti V, Gabet Y.** A new device for improving dental implants anchorage: a histological and micro-computed tomography study in the rabbit. *Clin Oral Implants Res.* 2016;27(8):935–942.

**Author information:**

- O. Dolkart, PhD, Director of the Orthopaedic Research Unit
- E. Kazum, MD, Shoulder Specialist
- Y. Rosenthal, MD, Shoulder Specialist
- G. Morag, MD, Director of the Sports Medicine Service
- O. Chechik, MD, Senior Shoulder Specialist
- E. Maman, MD, Director of the Shoulder Surgery Unit, Shoulder Unit, Division of Orthopaedic Surgery, Tel Aviv Sourasky Medical Center, Sackler Faculty of Medicine, Tel Aviv University, Tel Aviv, Israel.
- O. Sher, MD, Musculoskeletal Pathology Specialist, Pathology Institute, Tel Aviv Sourasky Medical Center, Sackler Faculty of Medicine, Tel Aviv University, Tel Aviv, Israel.
- E. Yakobson, BSc, CEO, Magdent Ltd, Bnei Brak, Israel.

**Author contributions:**

- O. Dolkart: Performed the literature search, Designed the study, Analyzed and interpreted the data, Wrote the manuscript.
- E. Kazum: Designed the in vivo experiments, Performed the biomechanical testing, Interpreted the data.
- Y. Rosenthal: Designed the study, Collected, analyzed, and interpreted the data, Wrote the manuscript.
- O. Sher: Performed the histological assessment, Interpreted the data, Wrote the manuscript.
- G. Morag: Designed the in vivo experiments, Performed the biomechanical testing, Interpreted the data.
- E. Yakobson: Performed the literature search, Designed the study, Wrote the manuscript.
- O. Chechik: Performed the literature search, Designed the study, Analyzed and interpreted the data, Wrote the manuscript.
- E. Maman: Performed the literature search, Designed the study, Collected, analyzed, and interpreted the data, Wrote the manuscript.
- O. Dolkart and E. Kazum contributed equally to this work.

**Funding statement:**

- Funding for this study was provided by Magdent Ltd. The author or one or more of the authors have received or will receive benefits for personal or professional use from a commercial party related directly or indirectly to the subject of this article.

**Ethical review statement:**

- All procedures were approved by the Institutional Animal Care and Use Committee at the Tel Aviv Sourasky Medical Center.

© 2021 Author(s) et al. This is an open-access article distributed under the terms of the Creative Commons Attribution Non-Commercial No Derivatives (CC BY-NC-ND 4.0) licence, which permits the copying and redistribution of the work only, and provided the original author and source are credited. See <https://creativecommons.org/licenses/by-nc-nd/4.0/>.